

Cofilin mediates ATP depletion-induced endothelial cell actin alterations

Maria V. Suurna,¹ Sharon L. Ashworth,¹ Melanie Hosford,¹ Ruben M. Sandoval,¹
Sarah E. Wean,¹ Bijal M. Shah,¹ James R. Bamburg,² and Bruce A. Molitoris^{1,3}

¹Division of Nephrology, Department of Medicine, Indiana University, and ³Roudebush Veterans Affairs Medical Center, Indianapolis, Indiana; and ²Department of Biochemistry and Molecular Biology, Colorado State University, Fort Collins, Colorado

Submitted 11 May 2005; accepted in final form 13 January 2006

Suurna, Maria V., Sharon L. Ashworth, Melanie Hosford, Ruben M. Sandoval, Sarah E. Wean, Bijal M. Shah, James R. Bamburg, and Bruce A. Molitoris. Cofilin mediates ATP depletion-induced endothelial cell actin alterations. *Am J Physiol Renal Physiol* 290: F1398–F1407, 2006. First published January 24, 2006; doi:10.1152/ajprenal.00194.2005.—Ischemia and sepsis lead to endothelial cell damage, resulting in compromised microvascular flow in many organs. Much remains to be determined regarding the intracellular structural events that lead to endothelial cell dysfunction. To investigate potential actin cytoskeletal-related mechanisms, ATP depletion was induced in mouse pancreatic microvascular endothelial cells (MS1). Fluorescent imaging and biochemical studies demonstrated a rapid and progressive increase in F-actin along with a decrease in G-actin at 60 min. Confocal microscopic analysis showed ATP depletion resulted in destruction of actin stress fibers and accumulation of F-actin aggregates. We hypothesized these actin alterations were secondary to dephosphorylation/activation of actin-depolymerizing factor (ADF)/cofilin proteins. Cofilin, the predominant isoform expressed in MS1 cells, was rapidly dephosphorylated/activated during ATP depletion. To directly investigate the role of cofilin activation on the actin cytoskeleton during ischemia, MS1 cells were infected with adenoviruses containing the cDNAs for wild-type *Xenopus laevis* ADF/cofilin green fluorescent protein [XAC(wt)-GFP], GFP, and the constitutively active and inactive isoforms XAC(S3A)-GFP and XAC(S3E)-GFP. The rate and extent of cortical actin destruction and actin aggregate formation were increased in ATP-depleted XAC(wt)-GFP- and XAC(S3A)-GFP-expressing cells, whereas increased actin stress fibers were observed in XAC(S3E)-GFP-expressing cells. To investigate the upstream signaling pathway of ADF/cofilin, LIM kinase 1-GFP (LIMK1-GFP) was expressed in MS1 cells. Cells expressing LIMK1-GFP protein had higher levels of phosphorylated ADF/cofilin, increased stress fibers, and delayed F-actin cytoskeleton destruction during ATP depletion. These results strongly support the importance of cofilin regulation in ischemia-induced endothelial cell actin cytoskeleton alterations leading to cell damage and microvascular dysfunction.

ischemia; sepsis; microvascular dysfunction

MULTIPLE EVENTS LEADING TO organ damage occur during ischemia and sepsis. Ischemic injury leads to vascular endothelium damage with disruption of the permeability barrier, detachment, swelling, and “endothelial cell activation” resulting in microvascular dysfunction (30, 47). Endothelial cell damage may also lead to increased ischemic injury and slowing of the recovery process (47).

The structure, shape, and function of endothelial cells are maintained by a complex protein filament network that comprises the intracellular cytoskeleton (26, 51). Actin filament

bundles are organized as short stress fibers, and they form a continuous circumferential band at the periphery of the cell. Dynamic functions of the actin cytoskeleton, mediated through shifts in monomeric (G-actin) and filamentous (F-actin) actin levels, play an important role in cellular morphology and permeability of the vascular endothelium (22). Progressive disassembly and shortening of the microfilaments of endothelial cells were observed during ATP depletion, and rapid reassembly was seen during cell recovery (24, 25, 33). Previous *in vivo* studies have evaluated actin cytoskeletal changes during ischemic injury (31, 48). The physiological F-actin structure of endothelial and vascular smooth muscle cells was markedly altered by 30 min of renal clamp ischemia, with increases in F-actin aggregates observed in endothelial and vascular smooth muscle cells (31, 48).

Assembly and disassembly of actin filaments are modulated by numerous actin binding proteins. The actin-depolymerizing factor (ADF)/cofilin (AC) family of proteins, known regulators of actin dynamics (7), plays a primary role in actin alterations during ischemia (4, 44). Dephosphorylation activates these proteins to control actin assembly and disassembly rates and actin filament severing by pH-dependent mechanisms (7). Two protein kinase families, LIM kinase, LIMK1 and LIMK2, and testicular protein kinase, TESK1 and TESK2, phosphorylate cofilin at its NH₂-terminal serine residue to inactivate cofilin's F-actin depolymerizing and severing activities (3, 36, 49, 50). LIM kinase is activated by phosphorylation mediated by p21-activated kinase-1 (PAK1), p21-activated kinase-4 (PAK4), and Rho-associated kinase (ROCK) (14, 16). PAK1 and PAK4 are activated by interactions with GTP-bound Rac/Cdc42 (14, 16), and ROCK is activated by interactions with GTP-bound Rho (36). TESK1 and TESK2 are stimulated by the integrin-mediated signaling pathway (41, 49, 50). LIMK1 and cofilin bind the scaffolding protein, 14–3–3 ζ , to modulate phosphatase-mediated phosphorylated (p)cofilin dephosphorylation (10, 21). Bone morphogenic protein receptor II (BMPR-II) binds LIMK1 and downregulates LIMK1 activity (18). Sling-shot phosphatases and chronophin (a member of the haloacid dehalogenase family) dephosphorylate and activate pcofilin (20, 27, 42).

Although the signaling pathways involved in ADF/cofilin regulation are becoming better defined, little is known about the specific intracellular molecular events that lead to endothelial cell dysfunction during ischemic injury. Therefore, the present studies were undertaken to define the mechanisms that lead to actin cytoskeletal alterations in response to ischemia in

Address for reprint requests and other correspondence: B. A. Molitoris, Div. of Nephrology, Indiana Univ. School of Medicine, 950 West Walnut St., Indianapolis, IN 46202-5116 (e-mail: bmolitor@iupui.edu).

The costs of publication of this article were defrayed in part by the payment of page charges. The article must therefore be hereby marked “advertisement” in accordance with 18 U.S.C. Section 1734 solely to indicate this fact.

endothelial cells. The importance of the ADF/cofilin family of proteins in actin cytoskeletal alterations during ischemic injury has been previously shown in epithelial cells (4). To determine the role of these proteins during ischemic injury of endothelial cells, studies using adenoviral vectors to introduce and express these regulating proteins were undertaken.

METHODS

Cell culture. All of the experiments were performed in the mouse pancreatic cell line MS1 [Mile Sven 1 cells purchased from American Type Culture Collection (ATCC), no. CRL-2279]. The MS1 cell line was maintained and expanded on plastic tissue culture dishes in DMEM (Sigma D-5523) containing 4 mM L-glutamine, 1.5 g/l sodium bicarbonate, 0.11 g/l sodium pyruvate, 4.5 g/l glucose, 5% FBS, 100 U/ml of penicillin, and 100 µg/ml of streptomycin, pH 7.4, at 37°C in 5% CO₂ incubators. The cells were grown on coverslips for fluorescent studies and on plastic dishes for protein extraction.

ATP depletion. ATP depletion was accomplished as previously reported (5). Before depletion, confluent MS1 cells were washed three times with HBSS (equilibrated at 37°C with 5% CO₂). Depleted medium (DMEM without glucose, pyruvate, or amino acids) was added to control plates, and depleted medium containing 0.1 µM antimycin A was added to the experimental plates. The cells were returned to the incubator for the ATP depletion periods of 5, 10, 15, 30, and 60 min (5).

Total cell extraction. For total cell protein extraction, SDS and chloroform/methanol extraction methods were used. In brief, MS1 cells were washed with cold PBS containing 0.5 mM CaCl₂ and 1.0 mM MgCl₂, pH 7.4, followed by the addition of extraction buffer (2% SDS, 10 mM Tris, pH 7.5, 10 mM NaF, 5 mM DTT, 2 mM EGTA, pH 8.0). The cells were scraped, boiled for 3–5 min, and briefly sonicated. This was followed by methanol/chloroform extraction (52). Protein pellets were air dried and resuspended in 2× or 4× sample buffer.

Quantification of F- and G-actin. MS1 cells were placed on ice, the medium was aspirated, and the cells were washed three times with HBSS. An extraction buffer [XB; 60 mM PIPES, 25 mM HEPES, 10 mM EGTA (PHEM), pH 6.9, 0.1% Triton X-100, 10 µg/ml chymostatin, leupeptin, antipain, and pepstatin A (CLAP), 0.5 mM PMSF, 0.1 mM DTT] was added to ATP-depleted cells, whereas an extraction buffer containing an ATP-regenerating system [(XB+ATP/RS; ATP-regenerating system-1 mM Na₂ ATP; A-5394, Sigma), 500 U creatine phosphokinase (C-3755, Sigma), and 10 mM creatine phosphate (P-6915, Sigma)] was added to control plates. Cells were scraped from plates, centrifuged, and the supernatants were separated from the cell pellets. The ATP-depleted and control cell pellets were resuspended in XB and XB+ATP/RS, respectively, and sonicated using a Branson Sonifier 450 (set on 3 in a scale of 1–10) with two to three 5-s bursts at 4°C. Supernatant and pellet samples were prepared in 2× Laemmli buffer for SDS-PAGE/Western blot analysis (39).

SDS-PAGE and Western blot analysis. Samples were dissolved in sample buffer, and protein concentration was determined by a quantitative filter paper dye-binding assay (38) or the Pierce Coomassie microtiter plate method. Samples of equal protein concentration were loaded into each lane and run on a 14% Tris-glycine minigel (Invitrogen, Carlsbad, CA) with SeeBlue molecular weight standards (Invitrogen). The samples were transferred onto polyvinylidene difluoride membranes (Millipore, Bedford, MA) using a Genie transfer unit (Idea Scientific, Minneapolis, MN) at 12 V for 2 h at room temperature. Membranes were blocked in blocking buffer (0.1 M NaCl, 0.01 M Tris·HCl, pH 7.4, 0.05% Tween 20 with 10% newborn calf serum; Hyclone, Logan, UT) for 30 min followed by incubation with primary antibody in blocking buffer (described below). The membranes were washed and then incubated in goat anti-rabbit (1:100,000 dilution) or goat anti-mouse (1:50,000 dilution) secondary antibody conjugated to horseradish peroxidase in blocking buffer. The membranes were

washed and incubated in SuperSignal ECL substrate (Pierce, Rockford, IL), imaged on Kodak X-ray film (Fisher Scientific, Chicago, IL), and densitometry was performed using an FX Imager with Quantity One software (Bio-Rad, Hercules, CA).

Primary antibodies. The following primary antibodies were used for Western blot analysis and indirect immunofluorescence detection: rabbit anti-ADF (12977, 1:1,000) (45); rabbit anti-phosphorylated ADF/cofilin that also recognizes phosphorylated XAC (1:1,000) (37); rabbit anti-XAC (1:1,000) (45); rabbit anti-LIMK1 (5 µg/ml in TBS; Chemicon, Temecula, CA); and mouse anti-actin C4 monoclonal antibody (1:3,000; Roche Diagnostics, Indianapolis, IN).

Immunoprecipitation. To evaluate for endogenous expression of LIMK1 in MS1 endothelial cells, immunoprecipitation was employed. Protein G-agarose beads were suspended in RIPA buffer (150 mM NaCl, 10 mM Tris, pH 7.5, 0.1% SDS, 1.0% Triton X-100, 1% deoxycholate, 5 mM EDTA) containing 10 µg/ml CLAP and 0.5 mM PMSF. The prepared beads were incubated on ice for 10 min with the primary antibody to LIMK1 (Chemicon). MS1 cells were washed two times with PBS and then rocked on ice for 10 min in RIPA buffer. The cells were removed, centrifuged, and the resulting cell extract was added to the protein G/anti-LIMK1 beads. This mixture was rotated at 4°C for 60 min, rinsed three times with RIPA buffer, and prepared in Laemmli buffer for gel electrophoresis. For the negative control, protein G-agarose beads without antibody were incubated with the cell extract. LIMK1-GFP (larger than LIMK1 by ~25 kDa) was expressed in mammalian cells and used as the positive control.

Adenoviral construct. Wild-type *Xenopus laevis* ADF/cofilin green fluorescent protein [XAC(wt)-GFP], the constitutively active mutant clone [XAC(S3A)-GFP], and the inactive mutant clone [XAC(S3E)-GFP] were constructed in the Clontech pHGFP-S65T vector by H. Abe, Chiba University, and generously shared with us (1). LIMK1 green fluorescent protein (LIMK1-GFP) clones were constructed by removing the LIMK1-coding region from the plasmid (8) and placing it into the multiple cloning site of a pAdv shuttle vector that was constructed by inserting two DNA fragments corresponding to base numbers 1–457 and 3328–8919 of the adenovirus type 5 genome (13) into the modified pBluescript II plasmid (Stratagene, Cedar Creek, TX). All fusion proteins were expressed under control of the immediate early promoter of the cytomegalovirus (CMV). The recombinant viruses were amplified in HEK-293 cells (CRL 1573, ATCC) (5).

Adenoviral cell infection. At 30–50% confluence, the MS1 cells were infected with either an adenovirus expressing GFP, XAC(wt)-GFP, the constitutively inactive mutant form XAC(S3E)-GFP, the constitutively active mutant form XAC(S3A)-GFP, or LIMK1-GFP at multiplicity of infection of 25 for the period of 18 h. The medium containing the virus was removed from the cells, cells were washed three times with PBS, new medium was applied, and protein expression was measured at 24, 48, and 72 h postinfection by Western blot analysis.

Fluorescence studies. Cells were fixed in 4% paraformaldehyde, permeabilized in 0.1% Triton X-100 in PBS, and blocked in PBS containing 2% BSA for 1 h at room temperature as previously described (5). F-actin was labeled with Texas red phalloidin (0.1 µg/ml; Molecular Probes, Eugene, OR), and the nuclei were labeled with Hoechst (2 µg/ml) for 1 h at room temperature (23). The fluorescence images were acquired with a Zeiss LSM 510 confocal microscope equipped with argon and helium/neon lasers using an inverted ×100, 1.4-numerical aperture oil-immersion objective.

RESULTS

ATP depletion induces actin polymerization and leads to changes in the actin cytoskeleton in MS1 cells. Fluorescence imaging studies of Texas red phalloidin-stained MS1 cells were undertaken to determine the effects of ATP depletion on the actin cytoskeleton. ATP depletion induced destruction of F-actin stress fibers and formation of “aggregated F-actin.”

Within 5 min of ATP depletion induction, an increase in Texas red phalloidin-stained actin aggregates was observed in the treated cells (Fig. 1A). Actin aggregates markedly increased with 15 and 30 min of ATP depletion. After 60 min of ATP depletion, there were less actin aggregates and bundled stress fibers, but numerous fine actin filaments were observed. Western blot studies were performed to quantify F-, G-, and total actin levels in MS1 cells following ATP depletion. Following 60 min of ATP depletion, total cellular F-actin increased with a corresponding decrease of G-actin (Fig. 1, B and C). These data are consistent with recent evidence showing a similar event in epithelial cells (6).

ATP depletion results in reduced pcofilin. Numerous studies have demonstrated that ADF/cofilin proteins have a role in rearrangement of the actin cytoskeleton (7, 43). Using specific antibodies to cofilin and ADF, cofilin was found to be the dominant AC protein in MS1 cells (~0.5% of the total cellular protein). To determine whether ATP depletion resulted in cofilin dephosphorylation/activation, time course studies were undertaken. Marked reductions in pcofilin levels were observed following 5 min of ATP depletion, and further ATP depletion led to a decrease in pcofilin concentration to undetectable levels (Fig. 2, A and B). There was no discernable variation in total cellular cofilin over 60 min of ATP depletion, indicating the decrease in pcofilin was a result of dephosphorylation and not due to cell loss or protein degradation (Fig. 2A).

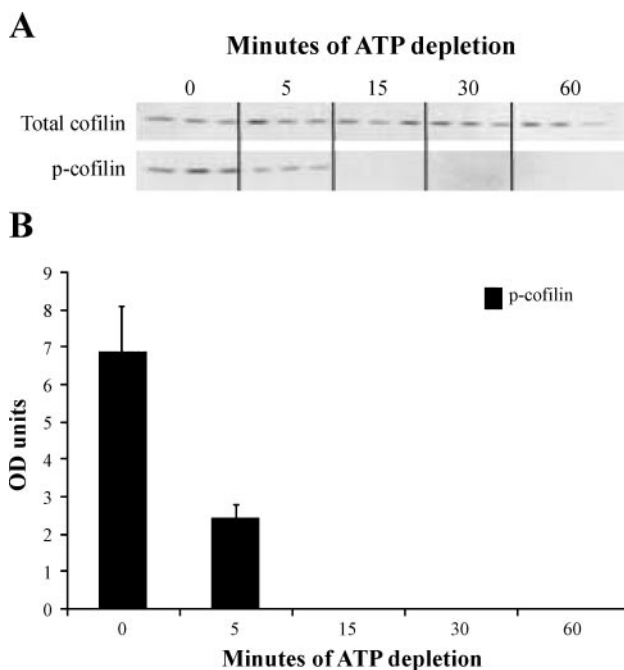


Fig. 2. ATP depletion dephosphorylates/activates pcofilin in MS1 cells. A: Western blot analysis of time course studies showing the effects of ATP depletion on total cofilin and phosphorylated (p) cofilin levels. B: statistical representation of the effects of ATP depletion on total pcofilin. OD, optical density.

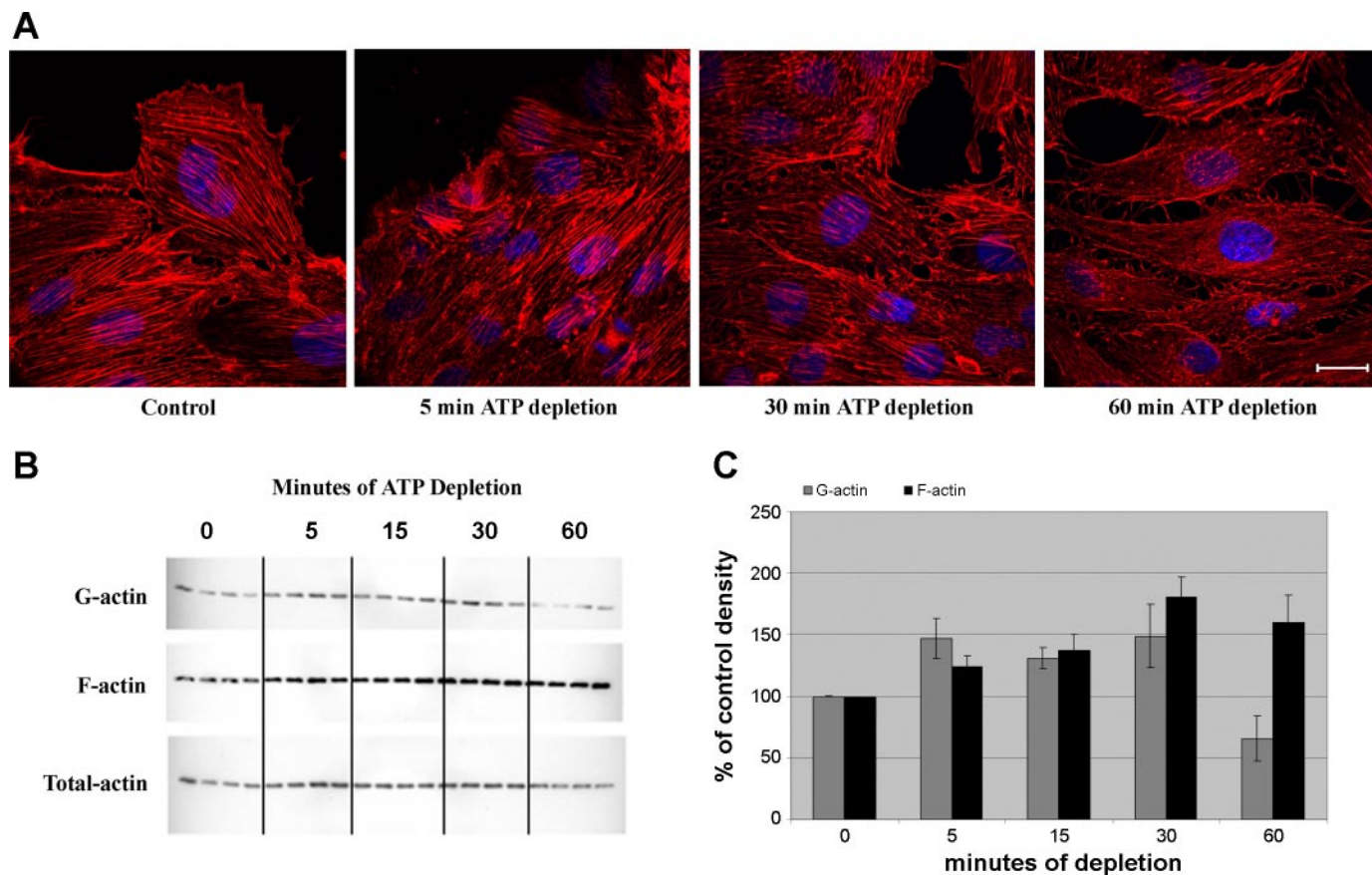


Fig. 1. ATP depletion induces actin polymerization in MS1 cells. A: effects of 5, 30, and 60 min of ATP depletion on the polymerization of actin. Polymerized actin is visualized by fluorescent imaging detecting Texas red phalloidin staining. B: Western blot analysis of the effect of ATP depletion on cellular F-actin, G-actin, and total actin levels. C: statistical representation of the effects of ATP depletion on cellular F- and G-actin levels. Scale bar = 20 μ m.

Expression of the ADF/cofilin isoform XAC(wt)-GFP leads to more rapid actin cytoskeleton changes following ATP depletion. ATP depletion in endothelial cells resulted in cofilin activation concurrent with F-actin rearrangement and polymerization. To directly evaluate the effect of ADF/cofilin on the actin cytoskeleton during ATP depletion, XAC(wt)-GFP, an ADF/cofilin isoform, was expressed in MS1 cells. Adenoviral constructs containing cDNAs for XAC(wt)-GFP, XAC(S3E)-GFP, XAC(S3A)-GFP, and GFP were used to induce transgene expression in endothelial cells. We observed variable adenoviral infection and GFP expression rates among the four constructs in endothelial cells. We did not observe any changes to the actin cytoskeleton in cells expressing XAC(wt)-GFP and GFP under physiological conditions 24 h postinfection (Fig. 3A), whereas we observed decreased stress fibers in some XAC(S3A)-GFP-expressing cells and increased stress fibers in the XAC(S3E)-GFP-expressing cells. Western blot studies demonstrated XAC(wt)-GFP expression increased with time postinfection (Fig. 3B), whereas corresponding total cellular actin levels in endothelial cells remained constant (Fig. 3C). These studies suggested XAC(wt)-GFP expression did not alter actin structures or total cellular actin levels under physiological conditions. However, following only 5 min of ATP depletion, fluorescent studies (Fig. 4) revealed a loss of F-actin stress fibers and rapid formation of F-actin aggregates in cells expressing XAC(wt)-GFP, whereas minimal F-actin aggregates were noted in cells expressing GFP alone. With ATP depletion, cells expressing XAC(S3A)-GFP demonstrated an even greater increase in actin aggregate formation and stress fibers loss compared with XAC(wt)-GFP-expressing cells, whereas cells expressing XAC(S3E)-GFP had increased stress fibers in number and density.

Western blot analysis was used in previous studies to demonstrate ATP depletion-induced dephosphorylation/activation of XAC(wt)-GFP (5). The present studies demonstrated that the levels of phosphorylated XAC(wt)-GFP decreased following 5 min of ATP depletion. This suggested ATP depletion-induced rapid activation of XAC(wt)-GFP in endothelial cells, which, in turn, correlated with rapid increases in cellular F-actin aggregates.

LIMK1 upregulates phosphorylation of ADF/cofilin in endothelial cells and slows down dephosphorylation during ATP depletion. To study the role of LIMK1 in endothelial cells, MS1 cells were infected with an adenoviral vector containing the cDNA of LIMK1-GFP. The effects of LIMK1-GFP expression were studied following 0, 24, and 48 h of expression. Western blot analysis demonstrated that as LIMK1-GFP expression increased over time, the levels of pcofilin also increased (Fig. 5, B and C). Endogenous LIMK1 expression was demonstrated with immunoprecipitation techniques (Fig. 5A). LIMK1-GFP (~25 kDa larger than LIMK1) was used as the positive control. During ATP depletion pcofilin was still present in LIMK1-GFP-expressing MS1 cells after 15 min of depletion, whereas pcofilin was undetectable beyond 5 min of ATP depletion in uninfected cells (Fig. 6, A and B). Therefore, cells expressing LIMK1-GFP were able to maintain phosphorylated/inactive cofilin for longer periods of time in response to ATP depletion.

LIMK1 expression prevents actin destruction and detachment of endothelial cells. Confocal imaging was used to compare effects of ATP depletion on MS1 cells under physi-

ological conditions and MS1 cells expressing LIMK1-GFP (Fig. 7). Cells expressing LIMK1-GFP had variable effects on the actin structure of physiological cells ranging from increased stress fibers in number and size to decreased stress fibers and formation of actin aggregates. However, following 30 min of ATP depletion, MS1 cells expressing LIMK1-GFP had better preserved and denser stress fibers than GFP-expressing control MS1 cells. Also, in this population of cells less cell-cell detachment was noted compared with 30 min of ATP depletion in GFP-expressing control cells. With 60 min of ATP depletion in cells expressing LIMK1-GFP, actin stress fibers were decreased and fine actin filaments were observed similar to what was seen in GFP-expressing control cells with 30 min of ATP depletion. Also, with 60 min of ATP depletion, LIMK1-GFP-expressing cells began to detach from neighboring cells but still did not demonstrate actin aggregate formation or cell-cell detachment as was observed in GFP-expressing control cells ATP depleted for 60 min.

DISCUSSION

Maintenance of adequate vascular flow is essential to maintain tissue perfusion and viability. During ischemic injury and septic shock, separation of endothelial tight junctions, loss of endothelial attachments to the basement membrane, endothelial blebbing, and endothelial necrosis have been observed (40, 48). Ischemia-induced endothelial cell injury results in activation of inflammatory cascades, increased vascular permeability, impaired vasodilation, obstructive microvascular thrombi, and white blood cell adhesion (34). These abnormalities result in reduced microvascular flow and continued ischemic injury (47). Improvement of renal function after renal ischemia by injection of a suspension of intact endothelial cells has demonstrated the importance of endothelial cell integrity for ischemic injury recovery (11, 15, 28, 32). Energy depletion and exposure to oxidants increased endothelial permeability and intercellular gap formation (24, 34). Also, increases in endothelial permeability were associated with internalization of VE-cadherin from endothelial adherens junctions (2, 29, 48). Energy depletion of endothelial cells leads to increased cell-cell separation and macromolecule permeability of the endothelial cell barrier due to rapid, but reversible disintegration of F-actin cytoskeletal structures (24).

Dynamic structure and function of the actin cytoskeleton involve the interaction of various actin binding proteins with F-actin. In particular, the ADF/cofilin family of proteins plays a significant role in actin cytoskeleton dynamics (7). ADF/cofilin proteins are a calcium-independent, actin binding protein family that in metazoans is regulated by phosphorylation (7). They bind actin monomers and filaments and stimulate actin filament severing and depolymerization in a pH-dependent manner (9). ADF/cofilin proteins function to enhance the off-rate of actin monomers at the pointed end of actin filaments and have actin-severing activities (12, 35). Activation and relocalization of ADF/cofilin to the apical domain during ischemia in renal tubular epithelial cells are coincident with disruption of the actin cytoskeleton (4, 44). In renal endothelial cells in vivo, ischemia induces a marked increase in F-actin polymerization and aggregation at the basal and basolateral aspects of the cells (48), which were associated with increased capillary permeability. In the present studies, ATP depletion

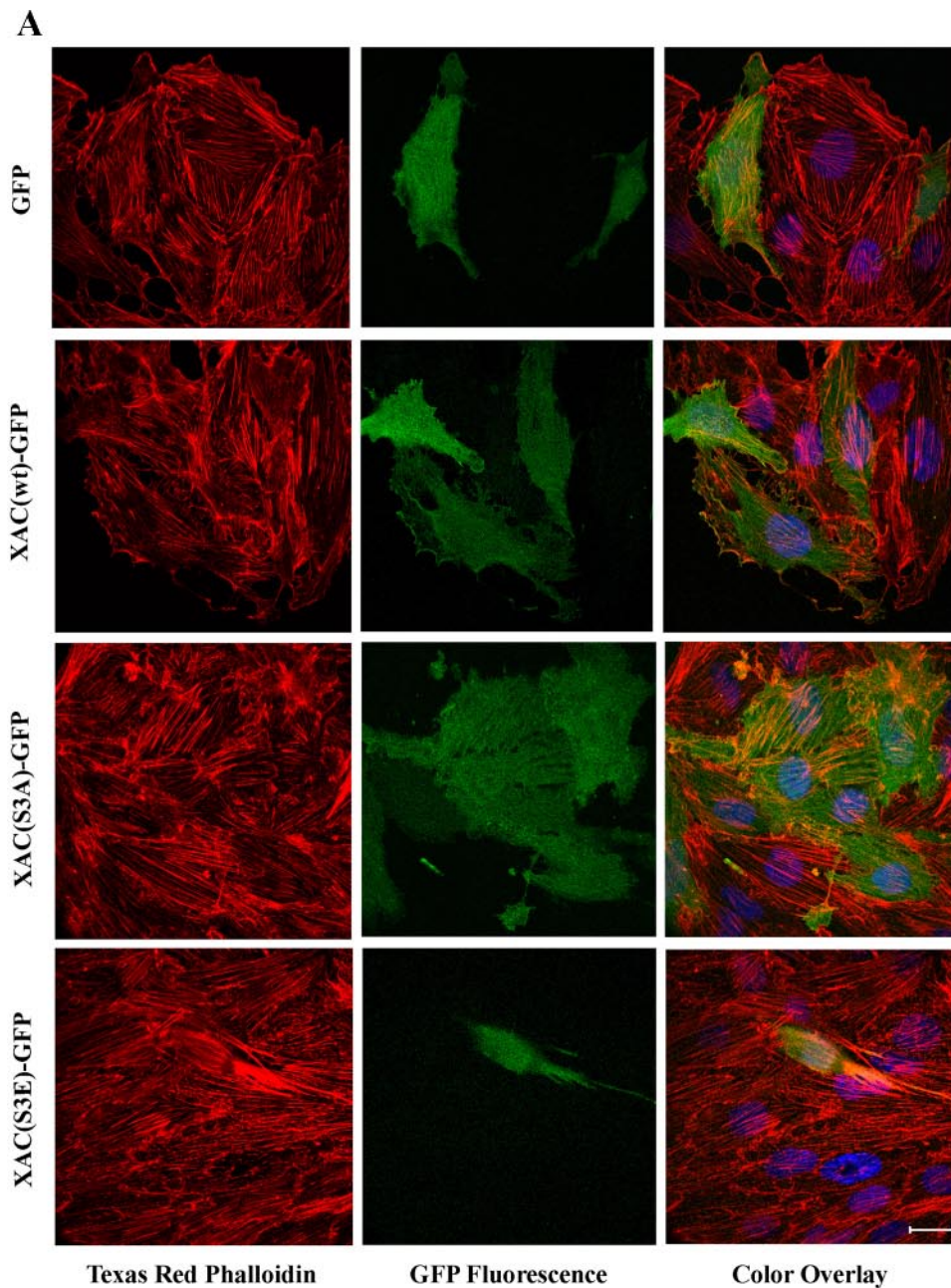
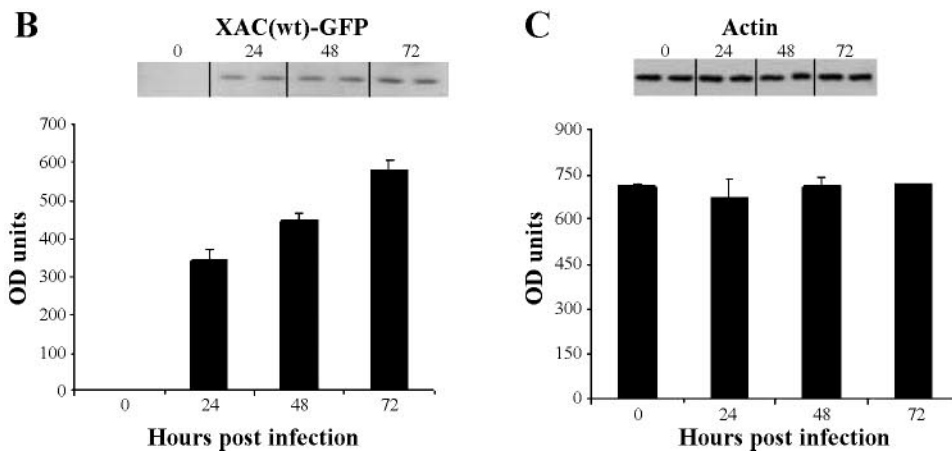


Fig. 3. XAC[wild-type (wt)]-green fluorescent (GFP) expression does not alter F-actin and total cellular actin. *A*: fluorescent studies of the effects of GFP, XAC(wt)-GFP, XAC(S3A)-GFP, and XAC(S3E)-GFP expression on actin cytoskeleton. *B*: Western blot demonstrating increasing XAC(wt)-GFP expression with time postadenoviral infection. *C*: Western blot showing corresponding actin levels with increased time postinfection with adenovirus containing XAC(wt)-GFP. Scale bar, 20 μ m.



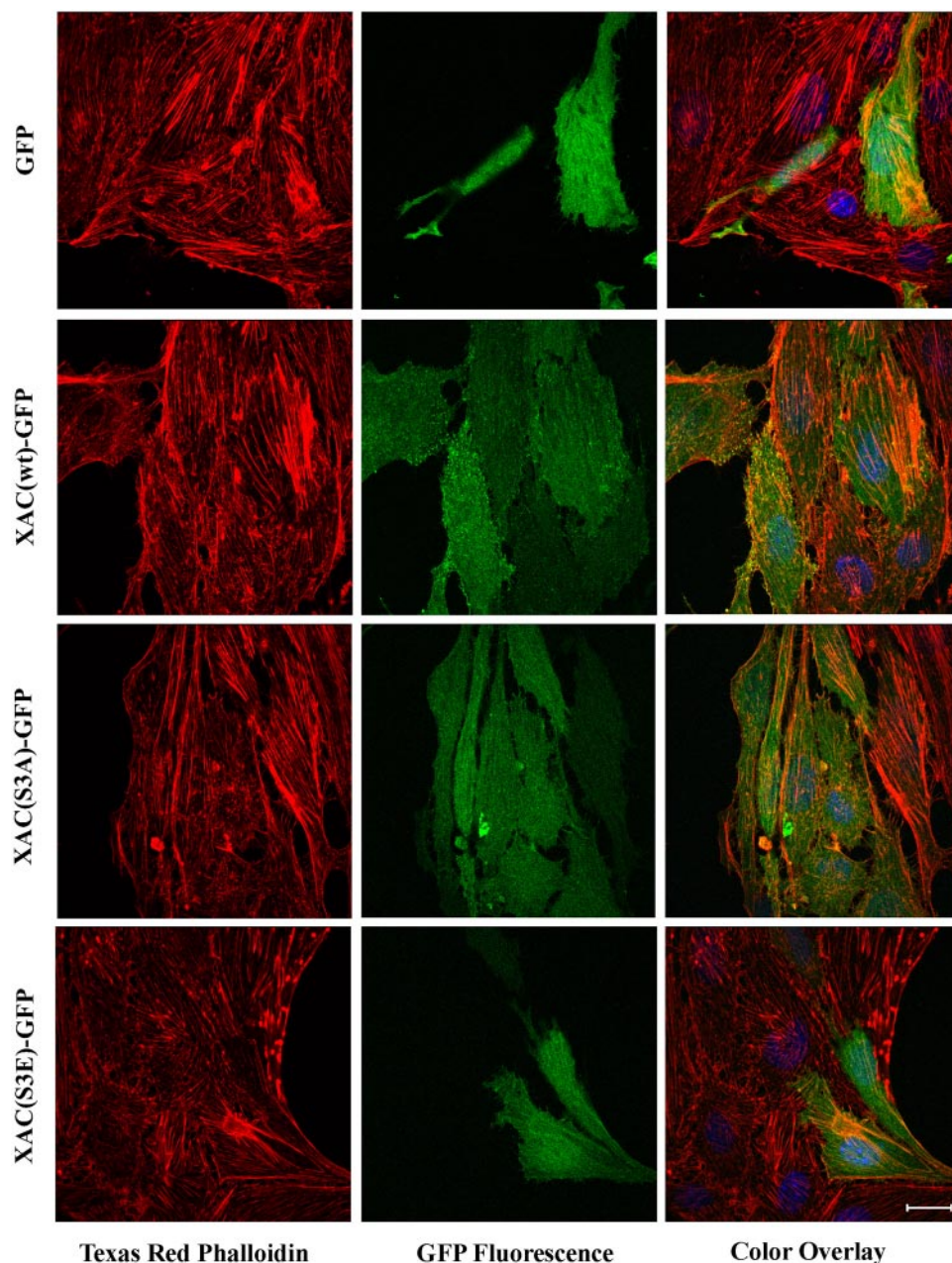


Fig. 4. Five minutes of ATP depletion result in rapid dephosphorylation/activation of XAC-GFP with F-actin depolymerization in cells expressing XAC(wt)-GFP. Fluorescent studies of F-actin following 5 min of ATP depletion in cells expressing GFP, XAC(wt)-GFP, XAC(S3A)-GFP, and XAC(S3E)-GFP. Minimal changes were observed in GFP- or XAC(S3E)-GFP-expressing cells, whereas XAC(wt)-GFP- and XAC(S3A)-GFP-expressing cells had decreased actin stress fibers and increased actin aggregates. Scale bar = 20 μ m.

induced cell-cell detachment and rapid aggregation of F-actin in endothelial cells, which are consistent with the results demonstrated in previous studies of endothelial cells (24, 30). ATP depletion also resulted in decreased G-actin and increased F-actin concentrations at 60 min, whereas the total cellular actin concentration remained unchanged. These actin alterations correlated with a decrease in cofilin, whereas the total cofilin concentration remained the same, demonstrating an increase in active cofilin via dephosphorylation. Phosphorylated cofilin was undetectable by Western blot analysis in endothelial cells beyond 5 min of ATP depletion. This implies early and rapid activation of cofilin in response to ATP depletion.

To directly investigate the effects of ADF/cofilin on cellular actin, we expressed XAC(wt)-GFP protein in endothelial cells using an adenoviral approach. Adenoviral-mediated expression

of cofilin was previously studied in human pulmonary artery endothelial cells (19). In this study, cofilin overexpression did not alter baseline endothelial cell permeability but reduced Sph-1-P-induced increases in cortical distribution of polymerized actin, resulting in a poorly developed cortical actin ring and limited the Sph-1-P barrier-enhancing effects. Expression of XAC(wt)-GFP further increased the rapid rate of actin redistribution and aggregation in response to ATP depletion compared with noninfected cells, suggesting that cofilin activation plays a contributing role in actin cytoskeleton disruption during ischemia. We observed marked cytoskeletal alterations that included disruption of stress fibers, most likely secondary to F-actin depolymerization and severing, and accumulation of actin aggregates, which could be secondary to uncontrolled actin polymerization of newly released ADP-containing actin monomers (6). We believe destruction of actin surface mem-

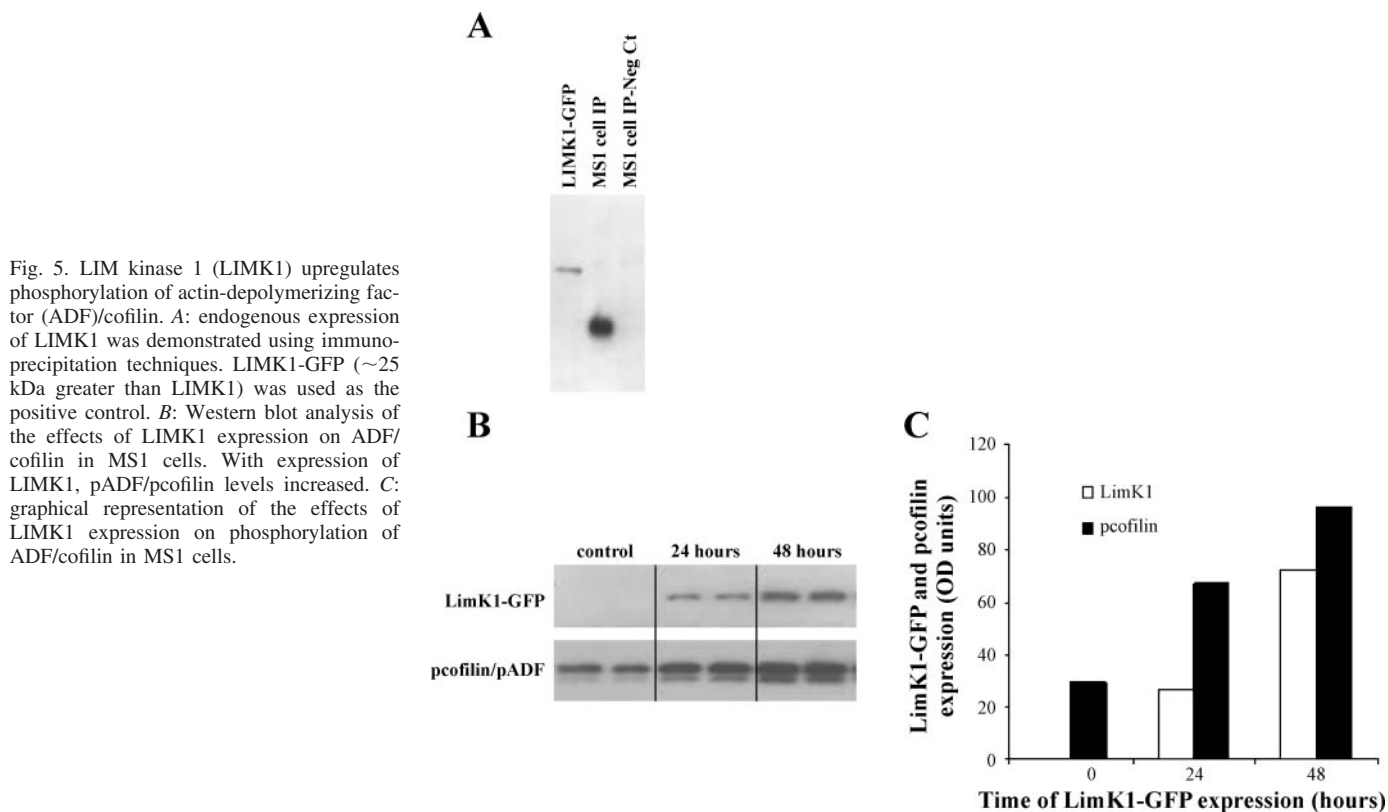


Fig. 5. LIM kinase 1 (LIMK1) upregulates phosphorylation of actin-depolymerizing factor (ADF)/cofilin. *A*: endogenous expression of LIMK1 was demonstrated using immunoprecipitation techniques. LIMK1-GFP (~25 kDa greater than LIMK1) was used as the positive control. *B*: Western blot analysis of the effects of LIMK1 expression on ADF/cofilin in MS1 cells. With expression of LIMK1, pADF/pcofilin levels increased. *C*: graphical representation of the effects of LIMK1 expression on phosphorylation of ADF/cofilin in MS1 cells.

brane interactions leads to cell-cell and cell-extracellular matrix detachment, resulting in increased microvascular permeability and detachment during ischemia (48).

To further explore the role of ADF/cofilin in regulating the actin cytoskeleton in endothelial cells, we introduced the ADF/cofilin-regulating protein LIMK1. LIM kinase proteins are known to phosphorylate ADF/cofilin at Ser3 (3, 53) and recently the phosphatase slingshot (SSH) as well as chronophin were shown to be responsible for ADF/cofilin dephosphorylation at the same site (20, 42). LIM kinase and SSH have the opposing effect on cellular cofilin activity, allowing for temporal and focal regulation of actin filament dynamics (17, 46). Previous *in vivo* studies in COS-7 cells demonstrated that LIM kinase induced changes in actin cables, with progressive accumulation of large aggregates of actin attributed to loss of cofilin function (16). In our studies, MS1 cells expressing LIMK1-GFP, under physiological conditions, were also noted to have aggregate accumulation and loss of stress fibers in some cells, whereas other MS1 cells expressing LIMK1-GFP showed increases in actin stress fiber number and thickness.

However, in the cells expressing LIMK1-GFP, less F-actin destruction was observed following 30 min of ATP depletion. At 60-min ATP depletion, stress fibers were replaced with a very fine actin network in both the LIMK1-GFP-expressing cells and adjacent noninfected cells. Biochemical analysis of LIMK1-GFP-expressing cells demonstrated that the phosphorylated form of ADF/cofilin persisted beyond 15 min of ATP depletion compared with the loss of pcofilin by 5 min in control cells. In these expression studies, not all cells in the culture expressed the LIMK1-GFP construct, so many noninfected cells were present in these cell cultures. It is expected that these noninfected cells undergo cofilin/ADF dephosphorylation in

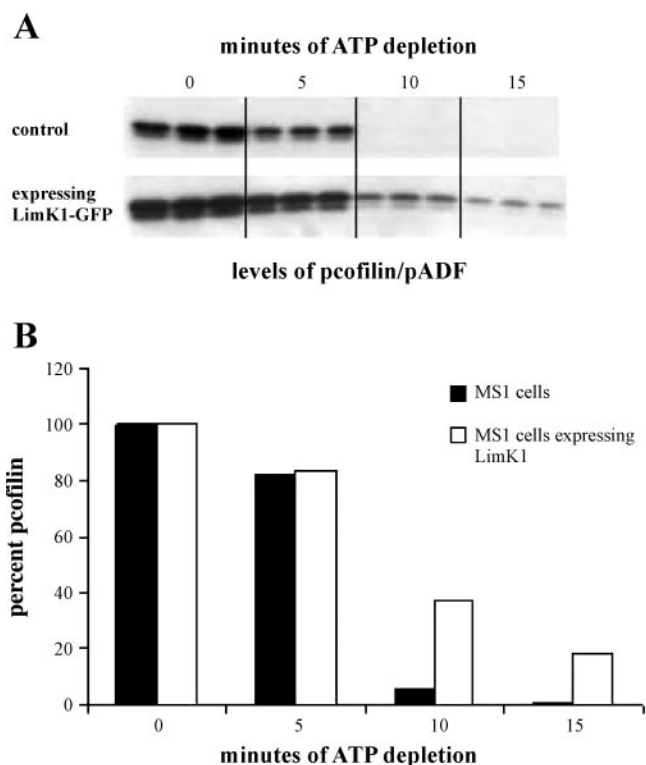


Fig. 6. LIMK1 inhibits dephosphorylation/inactivation of ADF/cofilin during ATP depletion. *A*: Western blot analysis of time course studies showing the effect of ATP depletion on the level of pcofilin/pADF in MS1 cells under physiological conditions and in cells expressing LIMK1. *B*: graphical representation of the effect of ATP depletion on pcofilin/pADF levels in MS1 cells in physiological condition and expressing LIMK1.

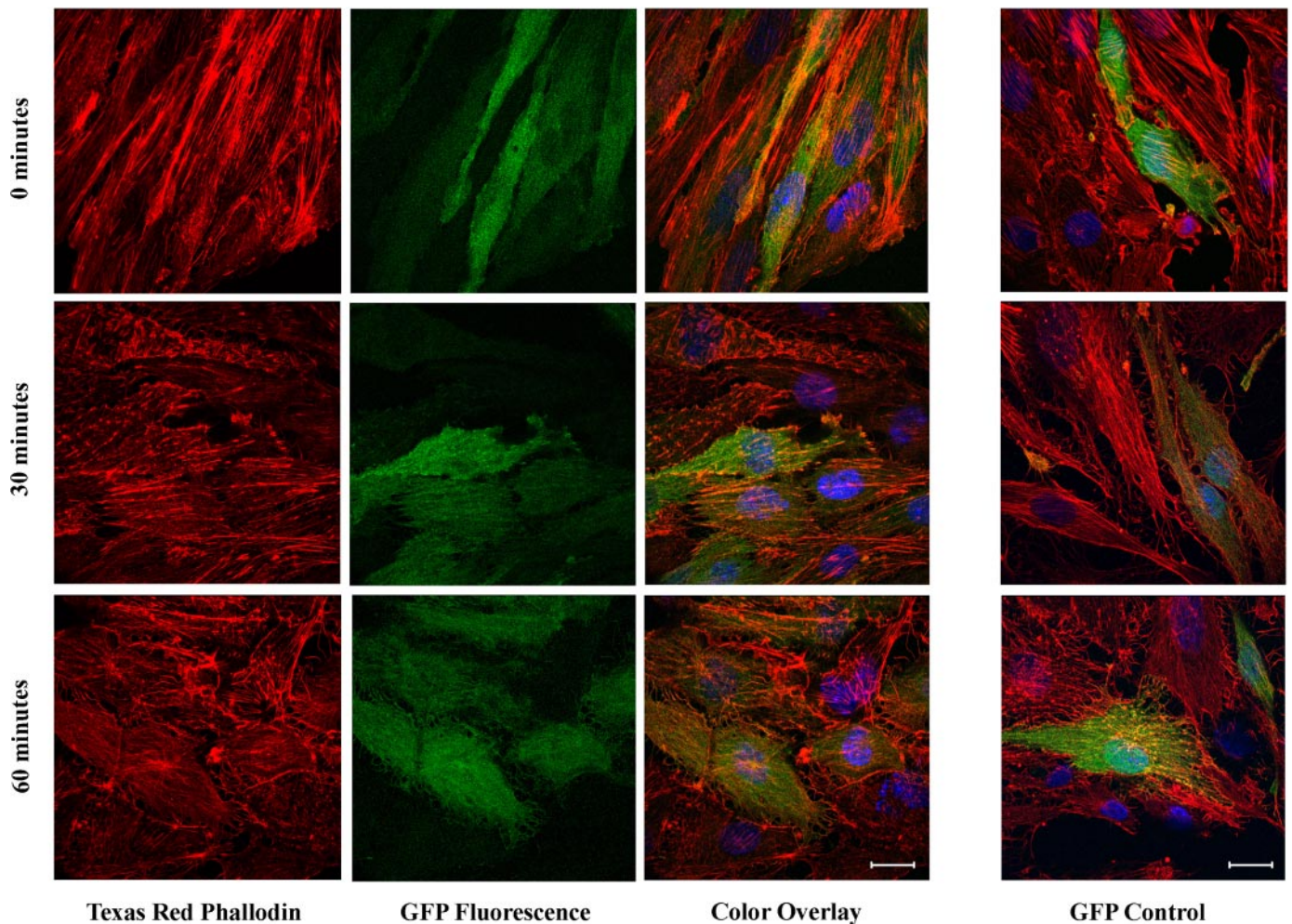


Fig. 7. LIMK1 expression prolongs cell-cell detachment and actin cytoskeleton destruction during ATP depletion. Fluorescent studies of MS1 cells expressing LIMK1-GFP F-actin changes after 30 and 60 min of ATP depletion. Under control conditions, stress fibers in some cells expressing LIMK1-GFP were increased in number and thickness, whereas other LIMK1-GFP-expressing cells showed some actin aggregates and decreased actin stress fibers compared with GFP-expressing control MS1 cells. However, with 30 min of ATP depletion, LIMK1-GFP-expressing cells still had stress fibers, whereas control GFP-expressing cells had decreased or no stress fibers, cell-cell detachment, and formation of fine actin aggregates. With 60 min of ATP depletion, the LIMK1-GFP-expressing cells demonstrated cell detachment, loss of stress fibers, and an increase in fine actin filaments similar to GFP-expressing control cells with 30 min of ATP depletion. Scale bar = 20 μm .

the same manner as is observed in control cells. The phosphorylated/inactivated cofilin present at 10 and 15 min in these samples most likely represents the population of cells in the culture that express the LIMK1-GFP transgene. These data support the hypothesis that LIMK1 exerts its protective role against ADF/cofilin's effects on the actin cytoskeleton during ATP depletion by phosphorylation and inactivation of ADF/cofilin proteins. Because the activity of LIMK1 is also known to be regulated by phosphorylation (16), it was expected that during prolonged ATP depletion, the levels of active LIMK1 would decline, leading to loss of its ability to phosphorylate ADF/cofilin.

It is important to note that expression of the constitutively active mutant XAC(S3A)-GFP in MS1 cells did not appreciably affect the integrity of the F-actin stress fibers under physiological conditions. However, ATP depletion of MS1 cells expressing this constitutively active mutant exhibited more damage to F-actin stress fibers and increased aggregate formation compared with XAC(wt)-GFP-expressing cells. This sug-

gests that an additional unknown mechanism other than cofilin regulation by phosphorylation/dephosphorylation may control the depolymerization and severing activity of cofilin in response to ATP depletion. Other actin binding proteins, such as tropomyosin, profilin, and AIP1, are known to influence the activity of cofilin. ATP depletion may affect the activity of these proteins and indirectly alter cofilin activity.

Our studies suggest that ADF/cofilin has a direct and concentration-dependent effect on alterations in actin cytoskeleton under ATP-depleted conditions. Actin aggregation and stress fiber destruction in response to ATP depletion are directly correlated to levels of exogenous ADF/cofilin expression. We have also demonstrated that LIMK1 expression delayed ADF/cofilin dephosphorylation/activation, providing a protective effect to the actin cytoskeletal structures. Regulation of ADF/cofilin activity in endothelial cells by LIMK1 demonstrates the vital role that ADF/cofilin plays in maintaining the structure of the actin cytoskeleton in endothelial cells. Further exploration of the intricate molecular pathways involved in ischemia-

induced cytoskeletal damage of endothelial cells and investigation into methods to counteract or slow down ADF/cofilin's effects on actin cytoskeleton destruction may provide insight into the mechanisms that would provide protection to endothelial cells during ischemic damage. In turn, this could result in preservation of the perfusion of vital organs.

REFERENCES

1. Abe H, Obinata T, Minamide LS, and Bamburg JR. *Xenopus laevis* actin-depolymerizing factor/cofilin: a phosphorylation-regulated protein essential for development. *J Cell Biol* 132: 871–885, 1996.
2. Alexander JS, Jackson SA, Chaney E, Kevil CG, and Haselton FR. The role of cadherin endocytosis in endothelial barrier regulation: involvement of protein kinase C and actin-cadherin interactions. *Inflammation* 22: 419–433, 1998.
3. Arber S, Barbayannis FA, Hanser H, Schneider C, Stanyon CA, Bernard O, and Caroni P. Regulation of actin dynamics through phosphorylation of cofilin by LIM-kinase. *Nature* 393: 805–809, 1998.
4. Ashworth SL, Sandoval RM, Hosford M, Bamburg JR, and Molitoris BA. Ischemic injury induces ADF relocalization to the apical domain of rat proximal tubule cells. *Am J Physiol Renal Physiol* 280: F886–F894, 2001.
5. Ashworth SL, Southgate EL, Sandoval RM, Meberg PJ, Bamburg JR, and Molitoris BA. ADF/cofilin mediates actin cytoskeletal alterations in LLC-PK cells during ATP depletion. *Am J Physiol Renal Physiol* 284: F852–F862, 2003.
6. Atkinson SJ, Hosford MA, and Molitoris BA. Mechanism of actin polymerization in cellular ATP depletion. *J Biol Chem* 279: 5194–5199, 2004.
7. Bamburg JR. Proteins of the ADF/cofilin family: essential regulators of actin dynamics. *Annu Rev Cell Dev Biol* 15: 185–230, 1999.
8. Bernard O, Ganiatsas S, Kannourakis G, and Dringen R. Kiz-1, a protein with LIM zinc finger and kinase domains, is expressed mainly in neurons. *Cell Growth Differ* 5: 1159–1171, 1994.
9. Bernstein BW, Painter WB, Chen H, Minamide LS, Abe H, and Bamburg JR. Intracellular pH modulation of ADF/cofilin proteins. *Cell Motil Cytoskeleton* 47: 319–336, 2000.
10. Birkenfeld J, Betz H, and Roth D. Identification of cofilin and LIM-domain-containing protein kinase 1 as novel interaction partners of 14–3-3 ζ . *Biochem J* 369: 45–54, 2003.
11. Brodsky SV, Yamamoto T, Tada T, Kim B, Chen J, Kajiya F, and Goligorsky MS. Endothelial dysfunction in ischemic acute renal failure: rescue by transplanted endothelial cells. *Am J Physiol Renal Physiol* 282: F1140–F1149, 2002.
12. Carlier MF, Laurent V, Santolini J, Melki R, Didry D, Xia GX, Hong Y, Chua NH, and Pantaloni D. Actin depolymerizing factor (ADF/cofilin) enhances the rate of filament turnover: implication in actin-based motility. *J Cell Biol* 136: 1307–1322, 1997.
13. Chroboczek J, Bieber F, and Jacrot B. The sequence of the genome of adenovirus type 5 and its comparison with the genome of adenovirus type 2. *Virology* 186: 280–285, 1992.
14. Dan C, Kelly A, Bernard O, and Minden A. Cytoskeletal changes regulated by the PAK4 serine/threonine kinase are mediated by LIM kinase 1 and cofilin. *J Biol Chem* 276: 32115–32121, 2001.
15. Day YJ, Huang L, McDuffie MJ, Rosin DL, Ye H, Chen JF, Schwarzschild MA, Fink JS, Linden J, and Okusa MD. Renal protection from ischemia mediated by A_{2A} adenosine receptors on bone marrow-derived cells. *J Clin Invest* 112: 883–891, 2003.
16. Edwards DC and Gill GN. Structural features of LIM kinase that control effects on the actin cytoskeleton. *J Biol Chem* 274: 11352–11361, 1999.
17. Endo M, Ohashi K, Sasaki Y, Goshima Y, Niwa R, Uemura T, and Mizuno K. Control of growth cone motility and morphology by LIM kinase and Slingshot via phosphorylation and dephosphorylation of cofilin. *J Neurosci* 23: 2527–2537, 2003.
18. Foletta VC, Lim MA, Soosairajah J, Kelly AP, Stanley EG, Shannon M, He W, Das S, Massague J, and Bernard O. Direct signaling by the BMP type II receptor via the cytoskeletal regulator LIMK1. *J Cell Biol* 162: 1089–1098, 2003.
19. Garcia JG, Liu F, Verin AD, Birukova A, Dechert MA, Gerthoffer WT, Bamburg JR, and English D. Sphingosine 1-phosphate promotes endothelial cell barrier integrity by Edg-dependent cytoskeletal rearrangement. *J Clin Invest* 108: 689–701, 2001.
20. Gohla A, Birkenfeld J, and Bokoch GM. Chronophin, a novel HAD-type serine protein phosphatase, regulates cofilin-dependent actin dynamics. *Nat Cell Biol* 7: 21–29, 2005.
21. Gohla A and Bokoch GM. 14–3-3 Regulates actin dynamics by stabilizing phosphorylated cofilin. *Curr Biol* 12: 1704–1710, 2002.
22. Gottlieb AI, Langille BL, Wong MK, and Kim DW. Structure and function of the endothelial cytoskeleton. *Lab Invest* 65: 123–137, 1991.
23. Herget-Rosenthal S, Hosford M, Kribben A, Atkinson SJ, Sandoval RM, and Molitoris BA. Characteristics of EYFP-actin and visualization of actin dynamics during ATP depletion and repletion. *Am J Physiol Cell Physiol* 281: C1858–C1870, 2001.
24. Hinshaw DB, Armstrong BC, Beals TF, and Hyslop PA. A cellular model of endothelial cell ischemia. *J Surg Res* 44: 527–537, 1988.
25. Hinshaw DB, Burger JM, Miller MT, Adams JA, Beals TF, and Omann GM. ATP depletion induces an increase in the assembly of a labile pool of polymerized actin in endothelial cells. *Am J Physiol Cell Physiol* 264: C1171–C1179, 1993.
26. Johnson-Leger C, Aurrand-Lions M, and Imhof BA. The parting of the endothelium: miracle, or simply a junctional affair? *J Cell Sci* 113: 921–933, 2000.
27. Kaji N, Ohashi K, Shuin M, Niwa R, Uemura T, and Mizuno K. Cell cycle-associated changes in Slingshot phosphatase activity and roles in cytokinesis in animal cells. *J Biol Chem* 278: 33450–33455, 2003.
28. Kale S, Karihaloo A, Clark PR, Kashgarian M, Krause DS, and Cantley LG. Bone marrow stem cells contribute to repair of the ischemically injured renal tubule. *J Clin Invest* 112: 42–49, 2003.
29. Kevil CG, Ohno N, Gute DC, Okayama N, Robinson SA, Chaney E, and Alexander JS. Role of cadherin internalization in hydrogen peroxide-mediated endothelial permeability. *Free Radic Biol Med* 24: 1015–1022, 1998.
30. Kuhne W, Besselmann M, Noll T, Muhs A, Watanabe H, and Piper HM. Disintegration of cytoskeletal structure of actin filaments in energy-depleted endothelial cells. *Am J Physiol Heart Circ Physiol* 264: H1599–H1608, 1993.
31. Kwon O, Phillips CL, and Molitoris BA. Ischemia induces alterations in actin filaments in renal vascular smooth muscle cells. *Am J Physiol Renal Physiol* 282: F1012–F1019, 2002.
32. Lin F, Cordes K, Li L, Hood L, Couser WG, Shankland SJ, and Igarashi P. Hematopoietic stem cells contribute to the regeneration of renal tubules after renal ischemia-reperfusion injury in mice. *J Am Soc Nephrol* 14: 1188–1199, 2003.
33. Loktionova SA and Kabakov AE. Protein phosphatase inhibitors and heat preconditioning prevent Hsp27 dephosphorylation, F-actin disruption and deterioration of morphology in ATP-depleted endothelial cells. *FEBS Lett* 433: 294–300, 1998.
34. Lum H and Roebuck KA. Oxidant stress and endothelial cell dysfunction. *Am J Physiol Cell Physiol* 280: C719–C741, 2001.
35. Maciver S, Zot H, and Pollard T. Characterization of actin filament severing by actophorin from *Acanthamoeba castellanii*. *J Cell Biol* 115: 1611–1620, 1991.
36. Maekawa M, Ishizaki T, Boku S, Watanabe N, Fujita A, Iwamatsu A, Obinata T, Ohashi K, Mizuno K, and Narumiya S. Signaling from Rho to the actin cytoskeleton through protein kinases ROCK and LIM-kinase. *Science* 285: 895–898, 1999.
37. Meberg PJ, Ono S, Minamide LS, Takahashi M, and Bamburg JR. Actin depolymerizing factor and cofilin phosphorylation dynamics: response to signals that regulate neurite extension. *Cell Motil Cytoskeleton* 39: 172–190, 1998.
38. Minamide LS and Bamburg JR. A filter paper dye-binding assay for quantitative determination of protein without interference from reducing agents or detergents. *Anal Biochem* 190: 66–70, 1990.
39. Minamide LS, Painter WB, Schevzov G, Gunning P, and Bamburg JR. Differential regulation of actin depolymerizing factor and cofilin in response to alterations in the actin monomer pool. *J Biol Chem* 272: 8303–8309, 1997.
40. Mutunga M, Fulton B, Bullock R, Batchelor A, Gascoigne A, Gillespie JI, and Baudouin SV. Circulating endothelial cells in patients with septic shock. *Am J Respir Crit Care Med* 163: 195–200, 2001.
41. Nakano K, Kanai-Azuma M, Kanai Y, Moriyama K, Yazaki K, Hayashi Y, and Kitamura N. Cofilin phosphorylation and actin polymerization by NRK/NESK, a member of the germinal center kinase family. *Exp Cell Res* 287: 219–227, 2003.

42. Niwa R, Nagata-Ohashi K, Takeichi M, Mizuno K, and Uemura T. Control of actin reorganization by Slingshot, a family of phosphatases that dephosphorylate ADF/cofilin. *Cell* 108: 233–246, 2002.
43. Pollard TD, Blanchoin L, and Mullins RD. Molecular mechanisms controlling actin filament dynamics in nonmuscle cells. *Annu Rev Biophys Biomol Struct* 29: 545–576, 2000.
44. Schwartz N, Hosford M, Sandoval RM, Wagner MC, Atkinson SJ, Bamburg J, and Molitoris BA. Ischemia activates actin depolymerizing factor: role in proximal tubule microvillar actin alterations. *Am J Physiol Renal Physiol* 276: F544–F551, 1999.
45. Shaw AE, Minamide LS, Bill CL, Funk JD, Maiti S, and Bamburg JR. Cross-reactivity of antibodies to actin-depolymerizing factor/cofilin family proteins and identification of the major epitope recognized by a mammalian actin-depolymerizing factor/cofilin antibody. *Electrophoresis* 25: 2611–2620, 2004.
46. Soosairajah J, Maiti S, Wiggan O, Sarmiere P, Moussi N, Sarcevic B, Sampath R, Bamburg JR, and Bernard O. Interplay between components of a novel LIM kinase-slingshot phosphatase complex regulates cofilin. *EMBO J* 24: 473–486, 2005.
47. Sutton TA, Fisher CJ, and Molitoris BA. Microvascular endothelial injury and dysfunction during ischemic acute renal failure. *Kidney Int* 62: 1539–1549, 2002.
48. Sutton TA, Mang HE, Campos SB, Sandoval RM, Yoder MC, and Molitoris BA. Injury of the renal microvascular endothelium alters barrier function after ischemia. *Am J Physiol Renal Physiol* 285: F191–F198, 2003.
49. Toshima J, Toshima JY, Amano T, Yang N, Narumiya S, and Mizuno K. Cofilin phosphorylation by protein kinase testicular protein kinase 1 and its role in integrin-mediated actin reorganization and focal adhesion formation. *Mol Biol Cell* 12: 1131–1145, 2001.
50. Toshima J, Toshima JY, Takeuchi K, Mori R, and Mizuno K. Cofilin phosphorylation and actin reorganization activities of testicular protein kinase 2 and its predominant expression in testicular Sertoli cells. *J Biol Chem* 276: 31449–31458, 2001.
51. Vestweber D. Molecular mechanisms that control endothelial cell contacts. *J Pathol* 190: 281–291, 2000.
52. Wessel D and Flugge UL. A method for the quantitative recovery of protein in dilute solution in the presence of detergents and lipids. *Anal Biochem* 138: 141–143, 1984.
53. Yang N, Higuchi O, Ohashi K, Nagata K, Wada A, Kangawa K, Nishida E, and Mizuno K. Cofilin phosphorylation by LIM-kinase 1 and its role in Rac-mediated actin reorganization. *Nature* 393: 809–812, 1998.

